

Exciton spin state mediated photon-photon coupling in a strongly coupled quantum dot microcavity system

S. Reitzenstein,* S. Münch, P. Franek, A. Löffler, S. Höfling, L. Worschech, and A. Forchel
*Technische Physik, Physikalisches Institut and Wilhelm Conrad Röntgen Research Center for Complex Material Systems,
 Universität Würzburg, Am Hubland, D-97074 Würzburg, Germany*

I. V. Ponomarev and T. L. Reinecke
Naval Research Laboratory, Washington, D.C. 20735, USA
 (Received 2 July 2010; published 16 September 2010)

Semiconductor microcavities play a key role in connecting exciton states and photons in advancing quantum information in solids. In this work we report on coherent interaction between high quality microcavity photon modes and spin states of a quantum dot in the strong coupling regime of cavity quantum electrodynamics. The coupling between the photon and exciton modes is studied by varying the temperature, where the spin states are resolved with a magnetic field applied in Faraday configuration. A detailed oscillator model is used to extract coupling parameters of the individual spin and cavity modes, which shows that the coupling depends on features of the mode symmetries. Our results demonstrate an effective coupling between photon modes that is mediated by the exciton spin states.

DOI: [10.1103/PhysRevB.82.121306](https://doi.org/10.1103/PhysRevB.82.121306)

PACS number(s): 78.67.Hc, 42.50.Pq, 78.20.Ls, 78.55.Cr

Cavity quantum electrodynamics (cQED) of systems of quantum dots (QDs) coupled to semiconductor microcavities has attracted considerable attention, particularly after recent demonstrations of strong (coherent) coupling in them.^{1,2} These systems extend long-standing work on atoms in cavities to the solid-state environment. They provide an interface between the atomic-like states of quantum dots and photon polarization states (flying qubits) in quantum information. Two-level quantum emitters, given by excitons or spins, coupled coherently to optical modes of microcavities are the essential building blocks in solid-state quantum information.^{3,4} Optical manipulation of the quantum dot states coupled to cavity photons can provide two-qubit gates needed for logic operations⁵ and also distributed architectures for quantum communications and computing.⁶⁻⁹

Previous work on strong coupling in semiconductor microcavities has involved the interaction of spin degenerate excitons with the optical cavity modes. Strong coupling has been demonstrated using several microcavity structures,^{1,2,10} and tuning of the modes with temperature and electric fields has been implemented.^{11,12} Recently, we demonstrated tuning of the exciton-cavity interaction with a magnetic field through the diamagnetic shift and the exciton wave-function size.¹³ In addition, cQED in the strong-coupling regime has been exploited as a tool for QD spectroscopy and to identify a cavity mediated mixing of bright and dark exciton states.¹⁴ However, although spin-related light-matter interactions in cQED have been involved in a number of proposals,^{5,15,16} they have not yet been demonstrated experimentally in the field of quantum optics of solid state.

Here we study the interaction of the spin degree of freedom of excitons in InGaAs quantum dots with the photon cavity modes in pillar microcavities, and we address the question of how the polarization of the modes affects their coupling. The spin states are split with a Faraday magnetic field and their interactions with individual cavity modes are identified in magnetophotoluminescence experiments. The

interactions between individual spin-resolved exciton states and cavity modes are obtained by comparison with a detailed coupled oscillator model of the exciton and cavity modes. We find that the symmetries of these modes play an important role in the quantitative understanding of their coupling. An interesting feature of these results is a coherent coupling found between two photon modes via spin states of the quantum dots.

We investigate spin-related cQED effects in QD-micropillar systems using planar distributed Bragg reflector (DBR) samples grown by molecular-beam epitaxy. The high-quality microcavities contain 23 (27) mirror pairs of alternating quarter wavelength thick AlAs/GaAs layers in the upper (lower) DBR, respectively. A single low-density layer of In_{0.3}Ga_{0.7}As QDs is located at the antinode of the electric field in the central one- λ -thick GaAs layer.¹⁷ Quantum dots grown with 30% In concentration have been shown to have increased oscillator strengths that facilitate the observation of strong coupling in the QD micropillar system.¹ High- Q micropillar cavities with a diameter d_c of 1.6 μm are fabricated from the planar sample by means of high-resolution electron-beam lithography and electron cyclotron resonance (ECR) plasma etching. Details of the sample processing can be found in Refs. 18 and 19. The coupling of spin-polarized excitonic modes of the QD and the photonic modes of the micropillar cavity are investigated at cryogenic temperature by means of microphotoluminescence (μPL). cw photoluminescence experiments were performed with nonresonant excitation at 532 nm. A magnetic field varying between 0 and 5 T in the Faraday geometry was employed.

Spin-resolved light-matter interaction is explored by temperature-dependent μPL measurements at different magnetic fields. Figure 1 shows sets of μPL spectra of a 1.6 μm diameter micropillar at $B=0$ T [Fig. 1(a)] and at $B=3$ T [Fig. 1(b)] magnetic fields. On both panels a broad cavity peak has a distinctive left shoulder that can be deconvolved into two unequal Lorentzians (C_1 and C_2). Far from the re-

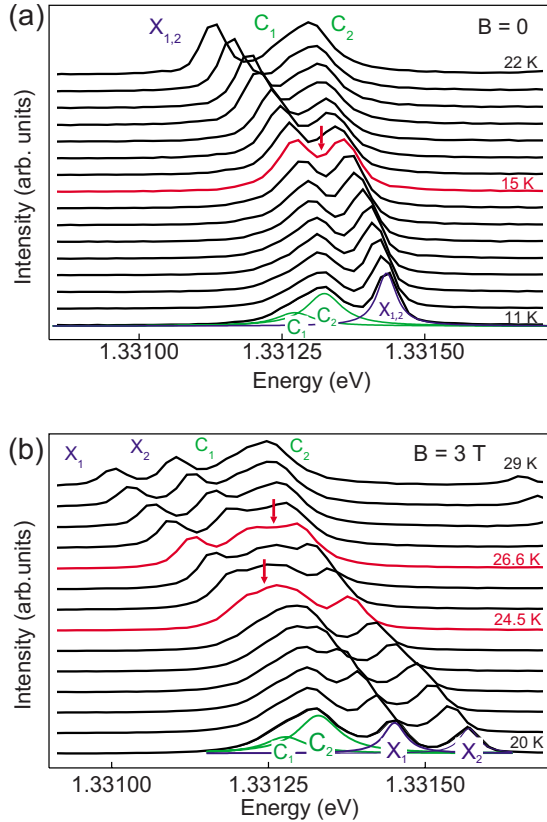


FIG. 1. (Color online) Temperature-dependent μ PL spectra of a 1.6 μ m diameter micropillar (a) at zero magnetic field and (b) at 3 T. The fundamental pillar cavity mode is split into two components C_1 and C_2 . At $B=0$ strong coupling between the photon modes and the nearly degenerate quantum dot exciton modes $X_{1,2}$ is identified by the avoided crossing of the associated lines with a mode's energy splitting of 86 μ eV. Coupling between the Zeeman split exciton lines (X_1 and X_2) and the cavity modes at $B=3$ T is seen in panel (b) and gives two interaction regions marked by arrows.

gion of light-matter coupling, their widths are approximately equal ($\Gamma_{C_{1,2}}=90$ μ eV). From line-shape fitting, the splitting between these modes was found to be $\alpha \approx 50$ μ eV. We have also performed angle-dependent polarization measurements of the cavity modes at zero magnetic field (not shown) which have confirmed this splitting. We found that these split modes are linearly polarized with Q factors of about 15,000. At $T=11$ K and zero magnetic field, a single QD exciton X peak represents two unresolved bright excitons X_1 and X_2 each with width $\Gamma_X=36$ μ eV. Polarization-dependent measurements of the exciton lines at $B=0$ T give a fine-structure splitting of $\beta=20$ μ eV.

At low temperatures, the exciton peaks are located on the high-energy side of the cavity modes in Fig. 1 so that temperature tuning can be used to study the light-matter coupling.¹ When the temperature is increased, the exciton has an avoided crossing with the cavity mode, which is a clear signature of the strong-coupling regime. The associated mode splitting at the resonance temperature of 15 K is 86 μ eV at $B=0$ T.

Spin-related effects come into play when a magnetic field splits the excitonic line into two components X_1 and X_2 . The

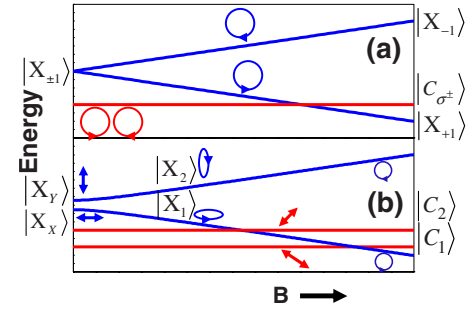


FIG. 2. (Color online) Schematic illustration of the energy dependences of the two excitons and the two cavity modes as a function of magnetic field at fixed temperature without light-matter coupling. (a) Two degenerate cylindrical cavity modes and two Zeeman split bright excitons in cylindrically symmetric QDs. (b) An asymmetry of the micropillar splits the two cavity modes by α and an asymmetry of the QD splits the bright exciton by β . At zero magnetic field, one observes two linearly polarized exciton modes separated by the fine-structure splitting. Increasing magnetic field gives rise to circular polarization of the excitons.

magnetic field also changes their polarizations and a total Zeeman splitting of $\Delta E_{Zeem}=117$ μ eV at $B=3$ T can be seen in the lowest trace of Fig. 1(b). Magnetic field dependent measurements at constant temperature give a diamagnetic coefficient of $\kappa=22$ μ eV/T² for the QD exciton, which reflects the extended electron-hole wave function of these large oscillator strength QDs.¹³

We are now in a position to address the coupling of spin-related excitonic emission lines with photonic modes of a microcavity at $B=3$ T. Both exciton lines shift through resonance with the cavity modes when the sample temperature is increased from 20 to 29 K. The smallest splitting in energy of the outermost emission lines is observed at about 25 K. At lower temperature a significant broadening and splitting (marked by an arrow) of the associated emission lines occurs when the X_1 component enters the interaction regime. In addition, a clear anticrossing behavior is observed at higher temperatures when the X_2 component shifts through resonance with the cavity mode. Both anticrossings indicate unambiguously the coherent cQED coupling with the Zeeman split exciton components in the spin-resolved cQED regime.

To understand the underlying physics of the measurements in Fig. 1(b) we first consider a situation without light-matter coupling. Figure 2 gives the schematic energy behavior and polarizations as a function of magnetic field for two cavity modes and two bright exciton modes. The upper panel shows the case in which the QD and the cavity each have cylindrically symmetric cross sections and the two cavity modes are degenerate.²⁰ The cylindrical symmetry of the QD preserves the total spin projection along the z axis. Then the two bright exciton states have right and left circular polarizations $|X_{+1}\rangle$, $|X_{-1}\rangle$. A nonzero magnetic field splits these two states.

In experiment we have seen that the cavity modes $|C_1\rangle$ and $|C_2\rangle$ have a splitting that we characterize by the parameter α and that the exciton modes at zero magnetic field have a splitting given by the parameter β . This suggests that these modes are each split by asymmetries [see Fig. 2(b)]. In the

case of the microcavity, this is attributed to a small ellipticity of the micropillar.¹⁸ Exciton states in InGaAs QDs are typically split at zero magnetic field by an asymmetry in QD structures. This gives linearly polarized states $|X_x\rangle$, $|X_y\rangle$ as illustrated in Fig. 2(b) with a fine-structure splitting parameter β .²¹ A strong magnetic field adds an additional splitting and tends to restore the circular polarization. At intermediate fields excitons are neither linearly nor circularly polarized, with a polarization governed by the ratio of parameters δ/β , where $\delta=g_L\mu_B B$ is the bare Zeeman splitting, and g_L is the Landé g factor. In the present experiment $\delta/\beta=6.25$ for $B=3$ T. The total splitting of two excitons is determined by the parameter $\tilde{\beta}=\sqrt{\beta^2+\delta^2}$.

We describe the system of four interacting modes by an effective Hamiltonian,

$$\hat{H}_{eff} = \begin{pmatrix} \tilde{E}_C & \frac{\alpha}{2} & g & 0 \\ \frac{\alpha}{2} & \tilde{E}_C & 0 & g \\ g & 0 & \tilde{E}_X - \frac{\delta}{2} & \frac{\beta}{2} \\ 0 & g & \frac{\beta}{2} & \tilde{E}_X + \frac{\delta}{2} \end{pmatrix}, \quad (1)$$

where $\tilde{E}_C=E_C-i\Gamma_C/2$, $\tilde{E}_X=E_X-i\Gamma_X/2$, and E_C , E_X are the central emission energies of the cavity mode and the exciton emission energy at $B=0$. The Hamiltonian is written in basis of cylindrically symmetric cavity modes and cylindrically symmetric QD excitonic states $|C_{\sigma^+}\rangle$, $|C_{\sigma^-}\rangle$, $|X_{+1}\rangle$, $|X_{-1}\rangle$. The parameters α and β determine the mixings of the two cavity modes and the two exciton modes, respectively. The energies and the linewidths Γ_C and Γ_X of the modes are obtained from the experiment depicted in Fig. 1(b) away from the interaction regime.²² To complete the description of the noninteracting modes in Eq. (1), we need the temperature dependences of the exciton and cavity modes. These are obtained by fitting the corresponding features in the experiment at zero magnetic field far from the interaction region by the forms $E_X(T)=A_X+B_X T-C_X T^2$ and $E_C=A_C-C_C T^2$.

The real and imaginary parts of the complex eigenenergies of the coupled modes as functions of T are calculated from Eq. (1) using only one free parameter, the coupling constant g between cavity and exciton states. The calculated mode energies are compared with the experimental values determined by performing least mean-square fits of the experimental results at $B=3$ T from Fig. 1(b) with four Lorentzian peaks. The best agreement was obtained for $g=38$ μeV . The corresponding energy dispersions of the four coupled modes are plotted in Fig. 3(a), where dotted lines give the energies of the uncoupled modes. It is seen that the theory (solid lines) describes the experimental data (dots) very well. In particular, the mode splittings in the interaction regimes (shaded areas) are nicely reproduced. We would like to note that the uncertainties of the mode energies are typical less than 3 μeV and that the size of the uncertainties in the energies are about the size of the data points.

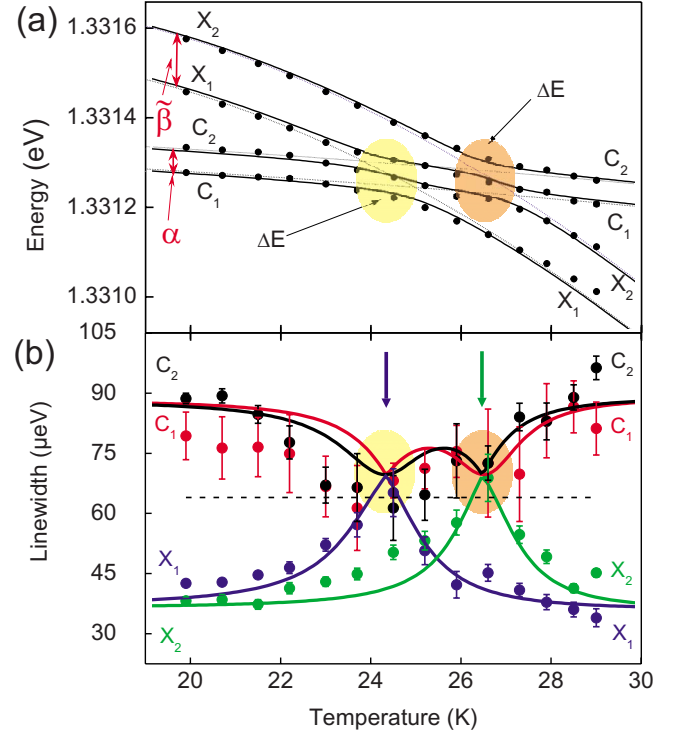


FIG. 3. (Color online) Energy dispersion and emission linewidths of the coupled modes at $B=3$ T as functions of temperature. (a) Experimental values (bullets) obtained by Lorentzian line-shape fitting of the data in Fig. 1(b) and calculated energy positions for $g=38$ μeV (solid lines). The black dashed lines indicate the peak energies for noninteracting modes, i.e., for $g=0$. The physical meaning of parameters α and $\tilde{\beta}$ in Eq. (1) is indicated. (b) Corresponding emission mode linewidths. In the interaction regions denoted by shaded areas, a pronounced mixing of three (two “cavity-like” and one “exciton-like”) modes occurs as a signature of the coherent light-matter interaction. The black dashed line indicates the expected value of linewidth crossings $(\Gamma_C+\Gamma_X)/2=64$ μeV for strong coupling of one exciton and a single photonic mode. The shift of the crossing points toward larger energies (at temperatures marked by arrows) indicates considerable involvement of the second photonic mode in the region of interaction.

The interactions between the four modes give rise to an anticrossing at the resonance of mode X_1 with C_1 and an anticrossing at the resonance of modes C_2 and X_2 [shaded areas in Fig. 3(a)]. The magnitude of each of these splittings is $\Delta E=86\pm 4$ μeV . It should be noted that splitting ΔE is composed partly of the coherent coupling given by g and partly by the (noncoherent) splitting between X_1 and X_2 (~ 20 μeV) and the splitting between C_1 and C_2 (~ 50 μeV). This is similar to the situation in which excitons from two different dots were coupled coherently by a single cavity mode in Ref. 23.

Additional insight into the physics of the coupled exciton spin-photon system can be obtained from the mode linewidths as a function of temperature and detuning. The calculated imaginary parts of the energy eigenvalues are shown in Fig. 3(b) along with the experimental results obtained from Lorentzian line-shape fitting of the data in Fig. 1(b). Pronounced mixing of the lines occurs for temperatures between

≈ 24 and ≈ 28 K. An exchange of linewidths between the X_1 transition and the C_1 cavity mode takes place at about 24.5 K (shaded region), which indicates coherent interaction in the strong-coupling regime.

From Fig. 3(a) we see that the splitting between the cavity modes C_1 and C_2 decreases for temperatures in the region of the crossing of the noninteracting modes C_1 and X_1 around 24.5 K. Specifically, the energy difference between the two lower lines in the figure for temperatures in this region is about $44 \mu\text{eV}$ compared to the mode splitting of $\alpha = 50 \mu\text{eV}$ at temperatures away from this anticrossing. This interesting feature results from interactions of the cavity modes with the exciton spin states from the quantum dot and is associated with an effective interaction strength which we estimate to be $6 \mu\text{eV}$. The exciton-mediated photon-photon interaction is consistent with the calculations of the coupled modes made from Eq. (1) and the physical mechanism for this coupling is the photon-exciton interaction given by the parameter g . This explanation is consistent with the behavior of the linewidths, which show considerable involvement of the C_2 mode [marked by the arrow in Fig. 3(b)] near this anticrossing. Indeed, the crossing point of the X_1 and the C_1 linewidths is shifted upwards compared to the expected value $(\Gamma_C + \Gamma_X)/2 = 64 \mu\text{eV}$ [indicated by a dashed line in Fig. 3(b)] for strong coupling with only a single photonic mode, an effect which is clearly observed for the experimental data at 26.6 K. This shows that the photonic character of the coupled modes is increased when two photon modes are involved in the spin-related light-matter interaction. The photon-photon coupling is interesting from a fundamental point of view, and nonlinear interactions mediated by quantum dots are also of considerable interest in connection with quantum communications and quantum information.²⁴

We note that the model in Eq. (1) gives accurate results under variation in only one free parameter, the coupling constant g . All other parameters Γ_C , Γ_X , $E_X(T)$, and $E_C(T)$ were obtained from experimental data away from the interaction regions. The only fitable parameter g was evaluated from data in the interaction region. g has a precise meaning from Eq. (1): it represents the coupling parameter between cylindrically symmetric cavity and QD basis states. The experimental cavity modes and exciton modes are obtained from the coupling of the cylindrically symmetric basis modes and the coupling parameters α and β .

In summary, we have addressed spin-related cQED effects in solid state by demonstrating strong (coherent) coupling between excitonic spin states and high-quality factor photon modes of a pillar microcavity structure. The spin states of excitons in InGaAs quantum dots are resolved with magnetic field and the coupled modes are observed in cw photoluminescence with nonresonant excitation. A detailed oscillator model is used to extract coupling parameters of the individual spin and cavity modes. Interestingly, we find a coupling of independent photonic modes via the excitonic transition in addition to the coupling between the spin states of the excitons and the cavity modes. These results represent important features of cQED and have high potential to pave the way for further studies on spin-related light-matter interaction and its application in quantum information science.

The authors acknowledge financial support by the Deutsche Forschungsgemeinschaft via the Research Group ‘‘Quantum Optics in Semiconductor Nanostructures,’’ the BMBF through the project ‘‘NanoQuit,’’ the State of Bavaria and the U.S. Office of Naval Research. We thank M. Emmerling and A. Wolf for technical assistance.

*stephan.reitzenstein@physik.uni-wuerzburg.de

¹J. P. Reithmaier *et al.*, *Nature (London)* **432**, 197 (2004).

²T. Yoshie *et al.*, *Nature (London)* **432**, 200 (2004).

³J. I. Cirac *et al.*, *Phys. Rev. Lett.* **78**, 3221 (1997).

⁴A. Imamoglu *et al.*, *Phys. Rev. Lett.* **79**, 1467 (1997).

⁵A. Imamoglu *et al.*, *Phys. Rev. Lett.* **83**, 4204 (1999).

⁶L. M. Duan and H. J. Kimble, *Phys. Rev. Lett.* **92**, 127902 (2004).

⁷W. Yao *et al.*, *Phys. Rev. Lett.* **95**, 030504 (2005).

⁸C. Press *et al.*, *Nature (London)* **456**, 218 (2008).

⁹I. Fushman *et al.*, *Science* **320**, 769 (2008).

¹⁰E. Peter *et al.*, *Phys. Rev. Lett.* **95**, 067401 (2005).

¹¹C. Kistner *et al.*, *Opt. Express* **16**, 15006 (2008).

¹²A. Laucht *et al.*, *New J. Phys.* **11**, 023034 (2009).

¹³S. Reitzenstein *et al.*, *Phys. Rev. Lett.* **103**, 127401 (2009).

¹⁴M. Winger *et al.*, *Phys. Rev. Lett.* **101**, 226808 (2008).

¹⁵C. Y. Hu *et al.*, *Phys. Rev. B* **78**, 085307 (2008).

¹⁶C. Bonato *et al.*, *Phys. Rev. Lett.* **104**, 160503 (2010).

¹⁷A. Löffler *et al.*, *Appl. Phys. Lett.* **86**, 111105 (2005).

¹⁸S. Reitzenstein *et al.*, *Appl. Phys. Lett.* **90**, 251109 (2007).

¹⁹S. Reitzenstein and A. Forchel, *J. Phys. D: Appl. Phys.* **43**, 033001 (2010).

²⁰L. Andreani *et al.*, *Phys. Rev. B* **60**, 13276 (1999).

²¹T. Takagahara, *Phys. Rev. B* **62**, 16840 (2000).

²²It is not possible to separate the homogeneous mode linewidths from inhomogeneity effects in these cw experiments.

²³S. Reitzenstein *et al.*, *Opt. Lett.* **31**, 1738 (2006).

²⁴W. Yao *et al.*, *Phys. Rev. Lett.* **92**, 217402 (2004).